Graph-Enhanced Electrical Impedance Tomography for Small-scale Object Localization

Yuxin Jin*, Yu-Hsiang Lin*, Vincenzo Maria Vitale†, Antonio Marino‡, Paolo Robuffo Giordano‡,

Marilena Vendittelli†, Claudio Pacchierotti‡, Sarthak Misra*§

*Surgical Robotics Laboratory, Department of Biomechanical Engineering, University of Twente,
Drienerlolaan 5, Enschede, The Netherlands
Emails: {y.lin-1, y.jin, s.misra}@utwente.nl
†Robotics Laboratory, Department of Computer, Control, and Management Engineering,
Sapienza University of Rome, Via Ariosto 25, Rome, Italy
Emails: {vitale.1697989, vendittelli}@studenti.uniroma1.it
‡CNRS, Univ Rennes, Inria, IRISA, Rennes, France
Emails: {antonio.marino, prg, claudio.pacchierotti}@irisa.fr
§Department of Biomaterials and Biomedical Engineering, University Medical Center Groningen, University of Groningen,
The Netherlands

***Abstract*—Over the recent years, miniature medical robots (MMRs) have garnered increasing attention from the research community due to their capability for precise therapeutic delivery and diagnostic procedures. Their compact form and exceptional agility allow them to access internal anatomical regions that traditional surgical tools cannot reach. To achieve effective control over MMR navigation, it is essential to accurately determine their position and movement, necessitating precise pose estimation. Consequently, unlocking the full clinical potential of MMRs hinges on the development of accurate and real-time tracking systems for these small-scale devices. Several imaging modalities have been investigated for this purpose, including magnetic resonance imaging (MRI) [1], [2], X-ray computed tomography (CT) [3], and clinical ultrasound [4], [5]. Each of these techniques provides distinct benefits while also presenting inherent drawbacks. While MRI offers excellent spatial resolution, it relies on a static and intense magnetic field, which is unsuitable for patients with metallic implants. CT imaging can achieve sub-millimeter resolution but raises concerns due to the ionizing radiation involved, affecting both patients and healthcare providers [6]. Ultrasound imaging stands out as a non-invasive and temporally precise method; however, it often suffers from image artifacts, particularly in complex and heterogeneous tissue environments. These limitations highlight the ongoing demand for alternative methods to track MMRs effectively.**

Electrical impedance tomography (EIT) presents a safe, non-invasive imaging solution capable of producing maps that reflect the conductivity distribution inside a medium. These impedance maps are reconstructed from voltage readings obtained through surface electrodes, while controlled currents are injected sequentially using selected electrode pairs. EIT has demonstrated its utility across a range of physiological monitoring applications, such as tracking respiration [7], brain function [8], and cardiopulmonary dynamics [9]. It has also shown potential in early breast cancer diagnosis by detecting electrical impedance changes associated with altered tissue structures [10]. These examples underscore EIT's capability to capture dynamic and non-uniform biological states, offering a promising alternative for localization in medical robotic systems. However, several engineering challenges remain before EIT can be broadly implemented for real-time tracking of MMRs.

A key limitation of EIT is its temporal resolution, which is constrained by both the rate of data acquisition and the efficiency of processing algorithms. The data collection rate is governed by how many current injection combinations are used and the sampling speed of the acquisition system. Meanwhile, processing speed depends on how effectively the inverse problem—estimating conductivity distributions from current injection patterns—is solved. In our system, each current injection pattern uses a pair of surface electrodes for current input and output. While increasing the number of such patterns improves spatial resolution through additional data, it also lengthens acquisition time. This creates a trade-off between spatial and temporal resolution. In the context of MMR tracking—where a small object moves within a much larger domain like the human torso—a method is needed that offers high spatial precision without compromising on frame rate.

In this work, we developed an integrated platform combining a custom-built EIT system and a robotic setup to autonomously acquire raw data for training a graph neural network (GNN)-based tracking model. The EIT configuration includes 16 evenly spaced electrodes, labeled ET_0 to ET_{15}, placed around the edge of an 80 mm diameter 3D-printed cylindrical workspace. Magnetically responsive objects are positioned inside the workspace and maneuvered using a permanent magnet mounted on a robotic arm. This movement is driven by magnetic attraction, which is generated by the spatial gradient in magnetic flux as the magnet is repositioned relative to the test object.

Electric current is delivered through chosen pairs of electrodes—referred to as stimulation patterns and denoted as $p_{i,j}$, where ET_i and ET_j represent the electrodes involved. The complete stimulation strategy, denoted ST, is defined as the collection of all such patterns necessary to map the impedance distribution:

$$ST = \{p_{i,j} \mid \forall i, j \in [0, 15]\}. \quad (1)$$

Voltage signals from all 16 electrodes are recorded while systematically varying the current injection pattern based on the

strategy ST, producing raw data used for accurately tracking the test object. This data is annotated using ground truth locations determined through a vision-based tracking system. The procedure is repeated at multiple workspace positions to build a diverse dataset for training the GNN model.

The raw data is initially formatted as a 3D matrix $\mathbf{X_t} \in R^{N \times n \times t}$, where N is the total number of stimulation patterns in ST, n is the electrode count, and t is the number of samples per electrode per pattern. Given a sampling rate of 500 Hz and a 50 Hz sinusoidal input signal lasting four cycles, t equals 40. Due to the complexity of this dataset, a dimensionality reduction is carried out before input to the GNN. First, the data is segmented based on stimulation pattern, and a Fast Fourier Transform (FFT) is applied. Then, for each group, the five frequency components with the highest amplitude are extracted to represent the dominant signal characteristics. These selected features preserve signal fidelity while reducing input complexity. All values are normalized to the range $[-1, 1]$ to minimize noise impact. These processed segments are treated as "nodes" within a graph, where "edges" connect nodes that share physical proximity—specifically, when their associated electrodes are adjacent and part of the same stimulation strategy.

This structured graph data is then processed using a graph neural network designed to learn the correlation between voltage signals and object position. The model starts with a multilayer perceptron (MLP) that adjusts the input vector from its initial 80 dimensions (derived from 16 electrodes × 5 FFT features) to fit the Graph Attention Network (GAT) input size. The data then flows through two GAT layers, which apply attention mechanisms to highlight the most relevant nodes for spatial learning. This structure improves the model's ability to detect spatial patterns within the graph. To balance feature expressiveness and generalization, we select 128 hidden units per layer—enough to capture complexity without risking overfitting due to excessive parameters. After feature extraction through GAT, a global max pooling operation condenses the learned graph features by selecting maximum activations across nodes and edges, ensuring salient spatial features are retained. The output is then passed to a final MLP, which converts the global representation into a 2D coordinate prediction for the micro-robot (128 × 2 output size). This architecture effectively combines spatial and temporal features for high-accuracy tracking.

The dataset comprises over 1000 labeled positions across the workspace for object with four different sizes respectively (6 mm, 8 mm, 10 mm, 12 mm), with a data split of 80% training, 10% validation, and 10% testing. The model's performance is assessed on the test set to evaluate its ability to generalize and precisely estimate the object's position, validating the effectiveness of the proposed tracking framework. The evaluation of the model performance is based on how well the model predicts the position of a given measurement in the test dataset. Using this method, we achieve accurate localization of a test object with a diameter down to 6 mm, which cannot be visualized using our current hardware and EIDORS solver. The proposed approach attains a median localization error of 2.88 mm with the 6 mm diameter object. Moreover, it takes 0.64 seconds to generate one frame with our approach (when the opposite strategy applies), which is significantly faster than using the EIDORS solver.

***Index Terms*—graph neural network, electrical impedance tomography (EIT), microrobotics, trajectory tracking**

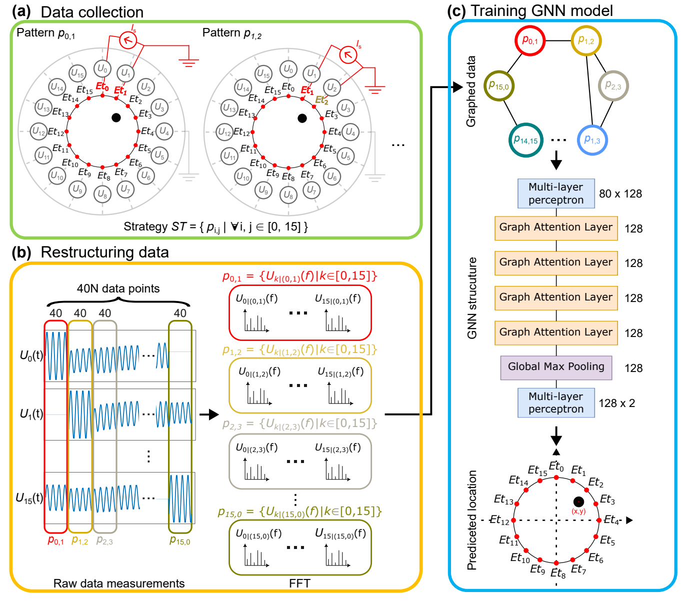

Fig. 1. **Schematic of the model training process** (a) The developed electrical impedance tomography (EIT) system consists of 16 electrodes (Et_0– Et_{15}) and a workspace. A stimulation signal is injected through a pair of selected electrodes. This pair of electrodes is termed a current injection pattern ($p_{\mathrm{i,j}}$), denoting the case when the electrode Et_{i} and electrode Et_{j} are selected. A current stimulation strategy (ST) is defined as a group of patterns required to reconstruct the impedance distribution of the workspace. Mathematically, a strategy can be expressed as $ST = \{p_{\mathrm{i,j}} \mid \mathrm{i,j} \in [0, 15]\}$. The data of one object position contains voltage measurements of all 16 electrodes ($U_{\mathrm{k}}, \mathrm{k} \in [0, 15]$) while sweeping all the current injection patterns in a chosen strategy. The raw data is labeled with the ground truth coordinates obtained from the vision-based image processing. (b) Restructuring the raw data into a graph gives syntax to the unorganized time series data. The shape of the initial data is $16 \times 40N$. This dimension is obtained from the measurements of 16 electrodes, each containing 40 data points per pattern, where N is the number of patterns in the strategy set, defined as $N = |ST|$. To reduce the dimension of the dataset, we first group the data points by the patterns and apply the Fast Fourier Transform (FFT) to each data group. Next, the first five components in the frequency domain are extracted for each group as new data. Next, we connect the data groups ("nodes") with "edges" if they fulfill the relationship we predefined. Hence, the raw data matrix can be restructured into a graphed dataset. (c) Once the graphed data structure is established, we feed the data into the graph neural network so that the relationship between the dataset and the ground truth location of the test object can be learned. The proposed neural network architecture consists of the following building blocks: an MLP layer to match the data dimensions, graph attention layers to learn the important features in a graphed dataset, and global max pooling to summarize the features so that they can represent the entire dataset and another MLP layer to predict the 2D locations.

References

[1] K. Belharet, D. Folio, and A. Ferreira, "Endovascular navigation of a ferromagnetic microrobot using mri-based predictive control," in *Proceedings of the IEEE/RSJ International Conference on Intelligent Robots and Systems (IROS)*, 2010, pp. 2804–2809.

[2] M. E. Tiryaki, S. O. Demir, and M. Sitti, "Deep learning-based 3d magnetic microrobot tracking using 2d mr images," *IEEE Robotics and Automation Letters*, vol. 7, no. 3, pp. 6982–6989, 2022.

[3] P. B. Nguyen, B. Kang, D. Bappy, E. Choi, S. Park, S. Y. Ko, J.-O. Park, and C.-S. Kim, "Real-time microrobot posture recognition via biplane x-ray imaging system for external electromagnetic actuation," *International Journal of Computer Assisted Radiology and Surgery*, vol. 13, pp. 1843–1852, 2018.

[4] F. Šuligoj, C. M. Heunis, S. Mohanty, and S. Misra, "Intravascular tracking of micro-agents using medical ultrasound: Towards clinical applications," *IEEE Transactions on Biomedical Engineering*, vol. 69, no. 12, pp. 3739–3747, 2022.

[5] K. Botros, M. Alkhatib, D. Folio, and A. Ferreira, "Fully automatic and real-time microrobot detection and tracking based on ultrasound imaging using deep learning," in *2022 International Conference on Robotics and Automation (ICRA)*. IEEE, 2022, pp. 9763–9768.

[6] J. L. Ryan, "Ionizing radiation: the good, the bad, and the ugly," *Journal*

of Investigative Dermatology, vol. 132, no. 3, pp. 985–993, 2012.

[7] V. Tomicic and R. Cornejo, "Lung monitoring with electrical impedance tomography: technical considerations and clinical applications," *Journal of thoracic disease*, vol. 11, no. 7, p. 3122, 2019.

[8] K. Y. Aristovich, B. C. Packham, H. Koo, G. S. Dos Santos, A. McEvoy, and D. S. Holder, "Imaging fast electrical activity in the brain with electrical impedance tomography," *NeuroImage*, vol. 124, pp. 204–213, 2016.

[9] C. Putensen, B. Hentze, S. Muenster, and T. Muders, "Electrical impedance tomography for cardio-pulmonary monitoring," *Journal of clinical medicine*, vol. 8, no. 8, p. 1176, 2019.

[10] Z. Rezanejad Gatabi, M. Mirhoseini, N. Khajeali, I. Rezanezhad Gatabi, M. Dabbaghianamiri, and S. Dorri, "The accuracy of electrical impedance tomography for breast cancer detection: A systematic review and meta-analysis," *The Breast Journal*, vol. 2022, no. 1, p. 8565490, 2022.